

**Comparison of the human gastric microbiota in hypochlorhydric states arising
as a result of *Helicobacter pylori*-induced atrophic gastritis, autoimmune
atrophic gastritis and proton pump inhibitor use**

**Bryony N. Parsons^{1#}, Umer Zeeshan Ijaz^{2#}, Rosalinda D'Amore³, Michael D.
Burkitt^{1,7}, Richard Eccles³, Luca Lenzi³, Carrie A. Duckworth¹, Andrew R.
Moore^{1,7}, Laszlo Tiszlavicz⁶, Andrea Varro¹, Neil Hall^{3,4,5} and D. Mark
Pritchard^{1,7*}**

*¹Department of Cellular and Molecular Physiology, Institute of Translational
Medicine, University of Liverpool, Crown Street, Liverpool, L69 3GE, UNITED
KINGDOM.*

*²University of Glasgow, Rankine Building, School of Engineering, Oakfield Avenue,
Glasgow G12 8LT, UNITED KINGDOM*

*³Centre for Genomic Research, Institute of Integrative Biology, University of
Liverpool, Crown Street, Liverpool, L69 7ZB, UNITED KINGDOM.*

⁴The Earlham Institute Norwich Research Park Norwich, NR4 7UH

*⁵School of Biological Sciences, University of East Anglia, Norwich Research Park,
Norwich, Norfolk, NR4 7TJ, UNITED KINGDOM*

⁶Department of Pathology, University of Szeged, HUNGARY

*⁷Royal Liverpool and Broadgreen University Hospitals NHS Trust, Prescot St,
Liverpool, L7 8XP, UNITED KINGDOM*

* Corresponding author D. Mark Pritchard Tel: +44 151 794 5772 Email:
dmpritch@liverpool.ac.uk

23 # These authors contributed equally

24 **Key words:** Gastric, hypochlorhydria, PPI, microbiota, atrophy, Helicobacter

25

ABSTRACT

Several conditions associated with reduced gastric acid secretion confer an altered risk of developing a gastric malignancy. *Helicobacter pylori*-induced atrophic gastritis predisposes to gastric adenocarcinoma, autoimmune atrophic gastritis is a precursor of type I gastric neuroendocrine tumours, whereas proton pump inhibitor (PPI) use does not affect stomach cancer risk. We hypothesised that each of these conditions was associated with specific alterations in the gastric microbiota and that this influenced subsequent tumour risk. 95 patients (in groups representing normal stomach, PPI treated, *H. pylori* gastritis, *H. pylori*-induced atrophic gastritis and autoimmune atrophic gastritis) were selected from a cohort of 1400. RNA extracted from gastric corpus biopsies was analysed using 16S rRNA sequencing (MiSeq). Samples from normal stomachs and patients treated with PPIs demonstrated similarly high microbial diversity. Patients with autoimmune atrophic gastritis also exhibited relatively high microbial diversity, but with samples dominated by *Streptococcus*. *H. pylori* colonisation was associated with decreased microbial diversity and reduced complexity of co-occurrence networks. *H. pylori*-induced atrophic gastritis resulted in lower bacterial abundances and diversity, whereas autoimmune atrophic gastritis resulted in greater bacterial abundance and equally high diversity compared to normal stomachs. Pathway analysis suggested that glucose-6-phosphate dehydrogenase and D-lactate dehydrogenase were over represented in *H. pylori*-induced atrophic gastritis versus autoimmune atrophic gastritis, and that both these groups showed increases in fumarate reductase. Autoimmune and *H. pylori*-induced atrophic gastritis were associated with different gastric microbial profiles. PPI treated patients showed relatively few alterations in the gastric microbiota compared to healthy subjects.

AUTHOR SUMMARY

Different conditions such as autoimmune atrophic gastritis and *Helicobacter pylori* associated atrophic gastritis are associated with different types of gastric cancer, specifically neuroendocrine tumours and adenocarcinoma. Both conditions result in reduced gastric acid secretion, potentially allowing non-*H. pylori* bacteria to colonise the stomach. However patients receiving proton pump inhibitors (PPI) experience similar levels of acid secretion, but do not develop gastric cancer. The aims of this study were to investigate the contribution of non-*H. pylori* microbiota to gastric tumour development in the presence of reduced gastric acid secretion and controls.

16S rRNA sequencing identified relatively few alterations in the gastric microbiota in patients receiving PPI therapy, despite reduced acid secretion, but more substantial alterations in those patients who had atrophic gastritis. Significant differences were also found between the patients who had atrophic gastritis of autoimmune and *H. pylori* associated types. Differences in biochemical pathways that potentially contribute to gastric tumorigenesis were also predicted.

This work increases understanding of the mechanisms involved in gastric tumour development, and demonstrates how non-*H. pylori* bacteria may be important. This work may eventually lead to the development of novel chemopreventive therapies for stomach cancer that are based on altering the composition of the gastric microbiota.

INTRODUCTION

Gastric adenocarcinoma is the third most common cause of cancer related mortality worldwide[1] and most cases are associated with chronic *Helicobacter pylori* infection. Gastric cancer usually develops via the premalignant condition of gastric atrophy, which is associated with the loss of acid-secreting parietal cells[2]. The resulting hypochlorhydria potentially leads to alterations in the composition of the gastric microbiota by providing a more favourable environment for colonisation. It is currently unclear to what extent the non-*H. pylori* gastric microbiota contributes towards gastric carcinogenesis. Although the hypochlorhydria associated with autoimmune atrophic gastritis also increases the risk of developing gastric adenocarcinoma[3], it is more frequently associated with the development of another tumour, the type I gastric neuroendocrine tumour (NET)[4]. However, hypochlorhydria does not always increase the risk of gastric tumour development, as observed following chronic proton pump inhibitor (PPI) use[5]. Therefore, factors in addition to hypochlorhydria affect gastric cancer risk and one of these could be the gastric microbiota.

Although originally thought to be sterile, several bacterial communities have been shown to survive in the normal human stomach[6]. Differences have also been observed depending upon *H. pylori* status[6]. There is now overwhelming evidence that certain bacteria influence cancer development. Potential mechanisms include altering the host immune system, exacerbating inflammation, or converting dietary nitrates to produce carcinogens such as N-nitrosamines and nitric oxide[7-13].

We therefore hypothesised that three stimuli which result in hypochlorhydria, namely *H. pylori*-induced atrophic gastritis, autoimmune atrophic gastritis and proton pump inhibitor use cause specific changes to the composition of the gastric microbiota. In

96 addition, the gastric microbiota that is present in these conditions contributes
97 towards the specific gastric tumour risk that is associated with each of these
98 hypochlorhydric states. We have used 16S rRNA sequencing to determine the
99 gastric mucosal microbiota profiles in patients with these causes of hypochlorhydria
100 and have compared these with samples obtained from healthy subjects and from
101 patients with *H. pylori*-induced gastritis, but no evidence of gastric atrophy.

RESULTS

Patient characteristics

Patients were selected from the larger cohort according to criteria defined in the methods section and Table 1. Characteristics of the selected patients are shown in table 1 and figure 1A. One sample from the normal stomach group and four from the PPI-treated group were subsequently excluded because sequencing showed the presence of >15% *H. pylori* despite this organism being undetected by conventional clinical tests (most likely due to the higher sensitivity of 16S rRNA sequencing compared to routine clinical tests). This is likely to be genuine *H. pylori* carriage since technical controls were included in each sequencing run and these controls showed lower diversity and levels of *H. pylori* than the samples (Figs 2 & 3). Ninety-five samples were therefore analysed. Negative extracts from the RNA extraction procedures, a water sample in the first PCR and a mock bacterial community were also sequenced.

Detection of Operational Taxonomic Units (OTUs)

In total 10,386 OTUs were identified. Extraction controls contained fewer OTUs than the patient samples, whilst the mock communities showed consistency between MiSeq runs (Figs 1-3). Despite the negative extracts being theoretically sterile, as expected they generated 16S signals due to known background reagent contamination[14]. Samples from the autoimmune atrophic gastritis group contained the largest number of OTUs, whilst all other patient groups were comparable (Fig 1B). Mock communities demonstrated the expected bacterial ratios (Fig 3B).

Bacterial diversity and abundance in the different hypochlorhydric states

Twenty-three known phyla were identified, mainly Proteobacteria, Firmicutes, Bacteroidetes, Actinobacteria, Fusobacteria and Cyanobacteria. Bacteroidetes, followed by Proteobacteria and Firmicutes were most common in normal stomachs, whereas samples from PPI-treated patients contained slightly more Firmicutes and fewer Bacteroidetes. The *H. pylori* gastritis and *H. pylori* atrophic gastritis samples were dominated by Proteobacteria (as *Helicobacter* itself is a member of this phylum), whilst biopsies from patients with autoimmune atrophic gastritis contained the largest proportion of Firmicutes compared to all other patient groups.

Alpha diversity

Diversity indices demonstrated that the microbiota in normal stomachs was significantly more diverse than in the stomachs of all other patient groups except for the patients who had autoimmune atrophic gastritis (Fig 2, all panels). Evaluation of evenness (by Pielou's evenness and Simpson) suggested that the samples from normal stomachs and from the stomachs of patients taking PPIs contained bacterial communities that were more equal in abundance than those in the other patient groups, which were more skewed (Fig 2). Calculations based on richness indicated that the samples from normal stomachs also contained the greatest number of different bacterial species compared to all other groups, whilst the two *H. pylori* infected groups (*H. pylori*-induced gastritis and atrophy) contained significantly fewer species.

Beta diversity

When beta diversity was explored using nonmetric distance scaling (NMDS), patient groups clustered predominantly by bacterial abundance (Fig 4). When *H. pylori* was removed from the analysis however, *H. pylori* gastritis patients no longer clustered separately by abundance from subjects with normal stomachs (Fig 4). Despite this, following removal of *H. pylori*, there was a significant difference in abundance for *H. pylori*-induced atrophic gastritis patients compared to normal stomachs, suggesting strongly that there are differences in the proportions of non-*H. pylori* bacteria in these subjects compared with others (Fig 4). Samples from patients who had autoimmune atrophic gastritis displayed the only significant differences in terms of the presence or absence of specific bacteria compared to other groups (Fig 4). This suggests that changes in the gastric bacterial community during hypochlorhydria usually involve changes in the relative proportions of bacteria that are already present, and only rarely involve the loss or gain of specific bacterial genera.

Comparisons between the microbiota profiles in the different patient groups and healthy controls

Normal stomach versus PPI treated patients

Patients receiving PPIs showed similar bacterial profiles to those found in the stomachs of normal subjects, despite having significantly higher serum gastrin concentrations (suggesting the presence of hypochlorhydria) (Figs 1A, 3 & S1). Nonetheless there were differences in the ranks of most abundant bacterial families. In normal (control) patients Prevotellaceae were the most abundant bacterial family (23%), followed by Streptococcaceae (10%), Paraprevotellaceae (7%) and Fusobacteriaceae (5%); amongst PPI-treated individuals Streptococcaceae (17%)

outranked Prevotellaceae (11%), Campylobacteraceae (5%) and Leptotrichiaceae (4%; Fig 3A). The only significant differences at genus level between these groups were decreases in *Actinobacillus* and *Tannerella* in the PPI-treated stomachs (Table S1). At the OTU level, *Cyanobacteria*, and *Streptococcus* were significantly increased in the PPI-treated samples, whereas *Prevotella*, *Porphyromonas*, *Treponema*, *Leptotrichiaceae*, *Haemophilus*, and *Fusobacterium* were significantly decreased compared to normal stomachs (Fig S2).

Very few differences were identified in co-occurrence network analyses when the microbiota in normal stomachs was compared to PPI-treated stomachs. The only observed difference was a negative correlation between *Helicobacter* and *Acinetobacter* in the PPI-treated samples, whereas this relationship was positively correlated in normal stomach biopsies (Figs 5A, S3A & Table S2A). Predicted pathway analysis showed no significantly different biochemical pathways between these two groups (Table S3).

Normal stomach versus H. pylori-induced gastritis

Unsurprisingly, the microbiota in the stomachs of patients who had *H. pylori*-induced gastritis consisted almost entirely of Helicobacteraceae (97%) (Fig 3). When compared to normal patients, *H. pylori*-induced gastritis patients showed a greater number of differences at the genus level than all other patient groups (Table S1). The majority of these differences resulted from reductions in the proportions of several bacterial genera within the *H. pylori* gastritis group. To ensure that the dominance of *H. pylori* did not skew the proportions of the other bacteria in a misrepresentational way, *H. pylori* OTUs were removed from the abundance table

followed by differential expression analysis on the remaining raw abundances. This analysis resulted in almost identical results to when *H. pylori* remained (Table S1). Due to the dominance of *H. pylori* in these patients, very few co-occurrence networks were identified, but positive correlations were observed between *Kocuria* and *Skermanella* in both groups (Figs 5A & B). Predicted pathway analysis suggested a reduction in several dehydrogenases in the stomachs of patients who had *H. pylori* gastritis (Table S3).

Normal stomach versus H. pylori-induced atrophic gastritis

The stomachs of patients who had *H. pylori*-induced atrophic gastritis were also dominated by Helicobacteraceae (62%), followed by Streptococcaceae (5%), Fusobacteriaceae (2%) and Prevotellaceae (2%) (Fig 3). At the genus level, several differences were observed between normal stomachs and the stomachs of patients with *H. pylori*-induced atrophic gastritis. These included decreases in the proportions of *Tannerella* (*E. coli*/*Shigella*/*Salmonella*, see supplementary methods), *Treponema*, and *Prevotella* in the *H. pylori*-induced atrophic gastritis group. The vast majority of these differences remained when *H. pylori* was removed from the analysis (Table S1). Prevotellaceae were generally lower in all patient groups compared to normal stomachs (Figs S1 and 3). As with the *H. pylori* gastritis group, the majority of these changes reflected decreases in the proportions of various bacterial genera within the *H. pylori*-induced atrophic gastritis group, with the only increase being in *Helicobacter* itself.

Co-occurrence networks were more complicated in *H. pylori*-induced atrophic gastritis patients compared to those subjects who had *H. pylori*-induced gastritis

(Figs 5B &D). Clear negative relationships were observed between *Helicobacter* and genera such as *Streptococcus*, whilst *Campylobacter*, *Prevotella*, *Haemophilus* and *Veillonella* were amongst the most well-connected and influential bacteria observed in the stomachs of *H. pylori* atrophic gastritis patients (Fig 5 and Table S2B). Predicted pathway analysis showed that several pathways were under-represented in the *H. pylori*-induced atrophic gastritis group, including succinate dehydrogenase (Table S3). Over-represented pathways included fumarate reductase (Table S3).

Normal stomach versus autoimmune atrophic gastritis

Streptococcaceae (38%) were the most dominant group identified in the stomachs of patients who had autoimmune atrophic gastritis, followed by Prevotellaceae (9%), Flavobacteriaceae (7%), Campylobacteraceae (7%), Enterobacteriaceae (5%) and Pasteurellaceae (5%). The stomachs of autoimmune atrophic gastritis patients contained a higher proportion of Streptococcaceae than all other patient groups (Fig 3) and were the only samples that showed complete loss or gain of bacteria rather than simply changes in bacterial proportions (Fig 4D). For example, the stomachs of autoimmune atrophic gastritis patients were colonised by *Gemella* and *Bosea* unlike any other patient group. Alterations in the relative proportions of other bacteria were also found in the stomachs of patients with autoimmune atrophic gastritis. These included increases in the proportions of *Streptococcus*, *Campylobacter* and *Haemophilus* (Table S1).

Few co-occurrence networks were identified, presumably due to the dominance of Streptococcaceae, although *Stenotrophomonas* and *Delftia*; and *Selenomonas* and *Pseudomonas* showed strong positive correlations (Fig 5D and Table S2B).

Predicted pathway analysis suggested that several pathways were over- or under-represented in the stomachs of patients who had autoimmune atrophic gastritis (table S3).

H. pylori gastritis versus *H. pylori*-induced atrophic gastritis

We investigated whether the microbiota in the stomachs of patients who had *H. pylori*-induced atrophic gastritis (which were likely to be hypochlorhydric as indicated by hypergastrinaemia) differed from that in patients who had *H. pylori* gastritis, normal gastric acid secretion and normogastrinaemia. No significant differences were identified at the genus level. However, several OTUs belonging to *H. pylori* were found more frequently in the *H. pylori*-induced atrophic gastritis group, possibly suggesting the presence of particular strains within this group (Table S4A). Interestingly, only two other OTUs differed in abundance between these groups, *Streptococcus mitis* and *Neisseria mucosa*. However, these did not remain significant once *H. pylori* was removed from the analysis. This suggests that the presence of atrophy does not result in extensive changes to bacterial communities in the stomach relative to the simple presence of *H. pylori*, but may result in specific differences in individual bacterial strains.

Comparisons between the gastric microbiota of individuals with hypochlorhydria of different aetiologies

Patients with *H. pylori*-induced atrophic gastritis and those receiving PPIs had similar fasting serum gastrin concentrations (median 100pM and 140pM respectively),

possibly suggesting similar degrees of hypochlorhydria (although *H. pylori* infection may have directly contributed to the hypergastrinaemia in the former group). In contrast patients with autoimmune atrophic gastritis were associated with higher fasting serum gastrin concentrations (median 800pM; Table 1). No direct association between fasting serum gastrin concentration and bacterial taxa was observed between the different groups (PERMANOVA Unifrac P=0.512, weighted Unifrac P=0.721 and Bray-Curtis P=0.556). This is reflected in the evidence that patients with *H. pylori*-induced atrophic gastritis and those receiving PPIs exhibited marked differences in 16S rRNA microbiota profiles, co-occurrence networks and predicted pathways, despite similar gastrin levels. And that patients with autoimmune atrophic gastritis showed similarities to individuals with *H. pylori*-induced atrophic gastritis by predicted pathway analysis, despite markedly different serum gastrin concentrations (Table S3).

Samples from patients with autoimmune atrophic gastritis contained significantly more *Streptococci* than all other groups (Fig 3 & Table S1). *Streptococcus* did not appear to be similarly increased in *H. pylori*-induced atrophic gastritis; this may have been due to the negative relationship observed between *Helicobacter* and *Streptococcus* identified in co-occurrence networks (Fig 5C).

Gastric biopsies from patients with autoimmune atrophic gastritis and those on PPIs both showed greater bacterial diversity than was observed in the stomachs of patients with *H. pylori*-induced atrophic gastritis (Fig 2). At the genus level, patients with autoimmune atrophic gastritis showed significant increases in *Tannerella*, *Dorea*, *Streptococcus*, *Fusobacterium* and *Campylobacter* compared to the patients with *H. pylori*-induced atrophic gastritis (Table S4B). The stomachs of PPI-treated patients also contained significantly higher proportions of *Fusobacterium* and

293 *Campylobacter* than the stomachs of *H. pylori*-induced atrophic gastritis patients.

294 Furthermore, patients receiving PPI treatment showed significantly higher
295 proportions of *Flavisolibacter* and *Dermacoccus* in their stomachs than autoimmune
296 atrophic gastritis patients, but significantly less *Paludibacter*, *Granulicatella*,
297 *Streptococcus*, and *Neisseria*.

298 Patients who had atrophic gastritis due to *H. pylori* or an autoimmune aetiology both
299 showed over-representation of several mutual pathways compared to controls (Table
300 S3). However, differences between the two groups were also observed. For
301 example, glucose-6-phosphate 1-dehydrogenase and D-lactate dehydrogenase
302 pathways were over-represented in the stomachs of patients who had *H. pylori*-
303 induced atrophic gastritis compared to those who had autoimmune atrophic gastritis
304 (Table S3).

305

DISCUSSION

Gastric samples obtained from subjects who had a normal stomach, no evidence of *H. pylori* infection and normogastrinaemia had the highest levels of microbial diversity. This is consistent with other reports of healthy populations showing more microbial diversity[15-17]. These samples also contained the greatest proportion of Prevotellaceae (23%) which corroborates previous research that reported normal stomachs contained 37% *Prevotella*, reducing to 28% in dyspeptic patients[18]. In general, the microbiota, co-occurrence networks and predicted pathways in samples from PPI-treated patients were similar to those in normal stomachs. This agrees with other reports that PPIs do not significantly influence the gastric microbiota[19, 20]. At the OTU level however, samples from PPI-treated patients contained significantly more *Streptococcus*. This has also been observed in gastric[20] and faecal samples from twins discordant for PPI use[21].

H. pylori gastritis, and to some extent *H. pylori*-induced atrophic gastritis samples were dominated by *H. pylori*. This observation may have been exacerbated by our use of RNA as opposed to DNA for sequencing, unlike many other publications. When these two techniques were directly compared, *H. pylori* abundance was found to be 19.9 times higher in RNA compared to DNA from gastric fluid samples, and was also more dominant in biopsies than gastric fluid[19, 22]. The use of RNA ensured that only viable bacteria were included in the analysis, giving a better indication of the taxa that are likely to be influencing the gastric environment. *H. pylori* colonisation was associated with a decrease in gastric bacterial diversity, and dominance of this organism, which is highly adapted to the gastric environment, has also been reported previously[6, 23, 24].

The majority of changes observed in *H. pylori* gastritis and *H. pylori*-induced atrophic gastritis samples were due to reductions in non-*H. pylori* bacteria. *H. pylori*-induced atrophic gastritis samples showed complex co-occurrence networks, unlike *H. pylori* gastritis which showed few connections, presumably related to the dominance of *H. pylori* itself in those samples. *Campylobacter*, *Prevotella*, *Haemophilus* and *Veillonella* were amongst the most influential genera in *H. pylori*-induced atrophic gastritis samples. These bacteria have been previously identified in oral and gastric samples[22]. The only differences found between the two *H. pylori* patient groups at the OTU level were increased abundances of specific *H. pylori* OTUs (possibly suggesting specific bacterial strains) and increased proportions of *Streptococcus mitis* and *Neisseria mucosa* in the atrophic group. The former species and latter genus have been identified from oral microbiota as potential biomarkers for pancreatic cancer[25]. *Neisseria* has been shown to produce large amounts of alcohol dehydrogenase, which produces the carcinogen acetaldehyde, and along with *H. pylori*'s high production of this enzyme, may also contribute to gastric carcinogenesis[26]. Some strains of Streptococcaceae have previously been shown to affect the outcomes of *H. pylori* infection. For example, *S. mitis* induces a coccoid state in *H. pylori*[27] and this may lead to unsuccessful antibiotic treatment and false negative diagnostic test results. Moreover, this coccoid form has been suggested to be more associated with gastric adenocarcinoma development than the spiral form[28, 29].

The stomachs of patients with autoimmune atrophic gastritis (who probably had the most profound reductions in acid secretion, as suggested by higher fasting serum gastrin concentrations), showed high bacterial diversity. Samples from this group also showed significantly higher proportions of *Streptococcus* than any of the other

groups. They also contained *Ruminococcus* and *Gemella* unlike any other patient group except *H. pylori*-induced atrophic gastritis, although they did not contain genera such as *Arthrobacter*, *Cupriavidus* and *Sneathia*. Therefore, bacterial communities were both lost and gained in this condition. Co-occurrence networks appeared to be disrupted by the overabundance of Streptococcaceae resulting in few connections.

The microbial profiles in the stomachs of patients with *H. pylori*-induced atrophic gastritis and autoimmune atrophic gastritis were quite different. In addition, pathways such as glucose-6-phosphate 1-dehydrogenase and D-lactate dehydrogenase were over-represented in the stomachs of patients with *H. pylori*-induced atrophic gastritis compared to autoimmune atrophic gastritis. Overexpression of these pathways has been associated with poorer prognoses in gastric cancer[30, 31]. Conversely, several other metabolic pathways such as fumarate reductase were increased in representation in patients with both autoimmune and *H. pylori* associated atrophic gastritis. Fumarate reductase is involved in the metabolism of some bacteria and is essential for colonisation by *H. pylori* in the mouse stomach[32-34]. Interestingly, succinate dehydrogenase (which has an opposite action to fumarate reductase) was found to be decreased in both atrophic gastritis groups compared to both the normal and PPI-treated samples. Lower levels of succinate dehydrogenase have previously been found in gastrointestinal tumours and parietal cells[35, 36]. PPI-treated patients showed more similarities in microbial diversity and abundance to the patients who had autoimmune atrophic gastritis, than to the patients who had *H. pylori*-induced atrophic gastritis.

The strengths of this study are the relatively large cohort of patients and the subsequently high numbers of samples sequenced. Weaknesses of the study

include a lack of dietary information recorded for the patients, and although patient groups had similar age and gender profiles it was not possible to specifically age/gender match them as priority was given to the strict criteria used to allocate patients to groups. Future studies are also needed to elucidate and confirm the predicted pathway analysis.

Conclusion

Our findings indicate that *H. pylori* colonisation and hypochlorhydria (other than that which was caused by PPI treatment) result in changes in gastric bacterial abundance and only rarely in loss/gain of bacteria. PPI treatment did not significantly alter the gastric microbiota from that of a normal stomach, despite serum gastrin concentrations being comparable to those found in patients with *H. pylori*-induced atrophic gastritis. Microbial patterns were not found to correlate with gastrin levels, although it should be noted that factors including *H. pylori* infection status may have confounded this relationship. Autoimmune atrophic gastritis resulted in a different, more diverse microbial pattern than that observed in the stomachs of patients who had *H. pylori*-induced atrophic gastritis. This may be due to differences in acid secretion between these conditions or other factors such as different immune profiles. Several biochemical pathways were represented in similar fashions in both atrophic gastritis groups. In particular, gastric-atrophy was associated with changes in the citric acid cycle (biochemical pathway that is known to be associated with gastric carcinogenesis) and our findings suggest that the microbiota may be an important contributor to this. The development of gastric cancer is multifactorial, and data from the present study suggest that the non-*H. pylori* microbiota may be a participating factor.

MATERIALS AND METHODS

Ethics

Acquisition of the biopsies used in this study was approved by Liverpool (08/H1005/37) and Cambridge East (10/H0304/51) Research Ethics Committees as previously described[37, 38]. All patients gave written informed consent.

Patients

One hundred gastric biopsy samples in 5 different groups were selected from a cohort of 1400 prospectively recruited patients who underwent diagnostic upper gastrointestinal endoscopy at Royal Liverpool University Hospital[37] and from 8 patients with type I gastric NETs who had been recruited to a clinical trial[38, 39] (Table 1). The patients in the 1400 cohort had the following characteristics: Females 57.5%, median age 60 years with an interquartile range 48-70 years and 98.4% were Caucasian. Overall more than half the cohort (52.3%) reported PPI use, 21.8% were positive for *H. pylori* infection by histology, and 43.3% were positive by serology. Patients were selected from this cohort according to the criteria described below and that are outlined in Table 1. None of the selected patients were taking PPIs, except those in the PPI treated group. In some patient groups (e.g. those with *H. pylori* associated atrophy and autoimmune atrophic gastritis) all samples which matched the inclusion criteria were sequenced, but for other groups (e.g. normal and PPI treated groups), subjects were chosen for inclusion based on the availability of tissue (as biopsy samples from this cohort have also been used for other studies).

427 **Table 1.** Summary of patient group characteristics

	Group	Total no. of samples	Number of females	Age (years)		BMI		<i>H. pylori</i> serology +ve	<i>H. pylori</i> histology /urease +ve	PPI use	Atrophic gastritis	Serum gastrin (pM)		Anti GPC/IF antibod
				Median	IQR	Median	IQR					Median	IQR	
1	Normal	20	13	46	30.5-58.7	24.5	21.2-26.8	0	0	-	-	22.5	17.5-28.5	- or ND
2	PPI treated	19	13	60	46-67	28.5	26.1-33.2	0	0	+	-	140	94-200	- or ND
3	<i>H. pylori</i> gastritis	22	11	57.5	47.7-64	27.4	23.3-27.1	22	22	-	-	21.5	17.4-28	- or ND
4	<i>H. pylori</i> atrophy	23	15	65	55-72	25.9	24.6-31.9	23	6	-	+	100	64-260	- or ND
5	Autoimmune atrophy	11	6	67	60-76	28.6	23.7-35	2	0	-	+	800	470-1050	+

428

429 ND= Not done

430 IQR= Interquartile range, 25% and 75%

431

432 Patients in the normal stomach group had a normal endoscopy, no evidence of *H.*
433 *pylori* infection by histology, rapid urease test or serology, were not taking a PPI and
434 were normogastrinaemic. Patients belonging to the *H. pylori* gastritis group were
435 positive for *H. pylori* by rapid urease test, histology and serology, had no histological
436 evidence of atrophic gastritis, were not taking a PPI and were normogastrinaemic.
437 Patients in the *H. pylori*-induced atrophic gastritis group showed histological
438 evidence of corpus atrophic gastritis and/or intestinal metaplasia, had no dysplasia
439 or cancer, were positive for *H. pylori* by serology, were not taking a PPI and were
440 hypergastrinaemic. Six out of the 23 patients in this group were also *H. pylori*
441 positive by urease test and/or histology. Details of histological Sydney scoring [40]
442 can be seen in supplementary figure 4. Patients in both *H. pylori* infected groups
443 showed higher scores in both antrum and corpus than patients in the normal
444 stomach and PPI treated groups. Patients in the autoimmune atrophic gastritis group

had histological evidence of atrophic gastritis, no evidence of *H. pylori* infection by rapid urease test or histology, positive anti-gastric parietal cell and/or intrinsic factor antibodies, were markedly hypergastrinaemic and 8 out of 11 also had grade 1 type I gastric NETs. Patients in the PPI-treated group were currently taking PPIs, had no evidence of *H. pylori* infection by serology, rapid urease test or histology, had no histological evidence of atrophic gastritis and were hypergastrinaemic (suggesting significant hypochlorhydria).

Samples

At least two biopsies per site were obtained from the gastric antrum and corpus for histopathology. Eight additional corpus biopsies were stored in RNA later immediately after removal and were extracted using a modified Tri- reagent protocol[41]. Briefly, samples were thawed and separated from RNA later, before being homogenised in Tri-Reagent® (Sigma-Aldrich, Gillingham, UK). Chloroform was added and the resulting clear aqueous layer was combined with isopropanol before centrifugation to produce a precipitated RNA pellet. This was washed with 75% and 100% ice cold ethanol before being allowed to dry and then resuspended in diethylpyrocarbonate (DEPC)-treated water (Sigma-Aldrich, Gillingham, UK). RNA was stored in ethanol at -80°C. Ethanol was removed and pellets were resuspended in DEPC-water prior to reverse transcription.

Gastrin assays

Serum gastrin concentrations were measured by radioimmunoassay (RIA) as previously described[42, 43]. Fasting serum gastrin concentrations were all <40pM in normogastrinaemic subjects and >40pM (with the majority >100pM) in hypergastrinaemic subjects.

Reverse Transcription

Samples and random primers were denatured together for 5 minutes at 65°C before Proto reaction mix and Proto enzyme from a ProtoScript® II First Strand cDNA Synthesis kit (NEB, E6560L) were added. Samples were then incubated at 25°C for 5 minutes, 42°C for 20 minutes, and 80°C for 5 minutes. Newly synthesised cDNA was then measured using a Qubit high sensitivity assay (ThermoFisher Ltd, Paisley, UK).

16S rRNA Sequencing

The 16S rRNA gene was targeted using V1-V2 (27F and 388R) primers[44] with slight modifications: forward primer 5'ACACTCTTTCCCTACACGACGC TCTTCCGATCTNNNNNAGAGTTTGATCMTGGCTCAG'3, reverse primer 5'GTGACTGGAGTTCAGACGTGTGCTCTTCCGATCTGCTGCCTCCCGTAGGAGT' 3. Primers were validated using a mock community described in supplementary methods. The following cycling conditions were used: initial denaturation 94°C for 5 minutes, followed by 10 cycles of denaturation at 98°C for 20 seconds, annealing at 60°C for 15 seconds, and elongation at 72°C for 15 seconds, followed by a final elongation step of 72°C for 1 minute. PCR amplicons were purified to remove excess primers, nucleotides, salts, and enzymes using the Agencourt® AMPure® XP system (Beckman Coulter Ltd, High Wycombe, UK). Purified amplicons were used in a second PCR reaction with the same conditions except with 20 cycles. This second step was used to add dual index barcodes. The PCR amplicons were purified as above. All PCR reactions used Kapa HiFi HotStart 2× master mix (Anachem Ltd, Bedfordshire, UK) and all primers were used at 10µM. Amplicon sizes were checked using a fragment analyser (Advanced Analytical, Ankeny, USA) and size

selection was performed using a Pippin prep (Sage Science, Beverly, USA). The quantity and quality of the samples in the final libraries were checked using a SYBR Green qPCR assay and the Illumina Library Quantification kit (Kapa) on a Roche Light Cycler LC480II, according to the manufacturer's instructions.

Prior to loading samples onto the MiSeq, PhiX was added (10-15%) to increase diversity, and samples were then denatured with NaOH according to the Illumina MiSeq protocol. ssDNA library fragments were diluted to a final concentration of 8pM. 600µl of ssDNA library was loaded into a MiSeq Reagent Cartridge and a 500-cycle PE kit v2 was used. Paired-end sequencing was performed according to the manufacturer's instructions (Illumina, SanDiego, CA, USA). Sequence analysis methodology is described in the supplementary methods. Reads were submitted to EBI short-read archive accession-PRJEB21104.

Statistical analysis

Details are described in the supplementary methods.

ACKNOWLEDGEMENTS

The authors wish to acknowledge all the patients and medical staff who participated in the study.

REFERENCES

1. Ferlay J, Soerjomataram I, Ervik M, Dikshit R, Eser S, Mathers C, et al. GLOBOCAN 2012 v1.0, Cancer Incidence and Mortality Worldwide: IARC CancerBase No. 11 [Internet]. Lyon, France: International Agency for Research on Cancer; 2013. Available from: <http://globocan.iarc.fr/>, accessed on 19/07/16.
2. Uemura N, Okamoto S, Yamamoto S, Matsumura N, Yamaguchi S, Yamakido M, et al. Helicobacter pylori infection and the development of gastric cancer. The New England journal of medicine. 2001;345(11):784-9. Epub 2001/09/15. doi: 10.1056/NEJMoa001999. PubMed PMID: 11556297.
3. Vannella L, Lahner E, Osborn J, Annibale B. Systematic review: gastric cancer incidence in pernicious anaemia. Aliment Pharmacol Ther. 2013;37(4):375-82. doi: 10.1111/apt.12177. PubMed PMID: 23216458.
4. Burkitt MD, Pritchard DM. Review article: Pathogenesis and management of gastric carcinoid tumours. Aliment Pharmacol Ther. 2006;24(9):1305-20. Epub 2006/10/25. doi: 10.1111/j.1365-2036.2006.03130.x. PubMed PMID: 17059512.
5. Song H, Zhu J, Lu D. Long-term proton pump inhibitor (PPI) use and the development of gastric pre-malignant lesions. The Cochrane database of systematic reviews. 2014;(12):CD010623. Epub 2014/12/03. doi: 10.1002/14651858.CD010623.pub2. PubMed PMID: 25464111.

- 530 6. Bik EM, Eckburg PB, Gill SR, Nelson KE, Purdom EA, Francois F, et al.
531 Molecular analysis of the bacterial microbiota in the human stomach. Proceedings of
532 the National Academy of Sciences of the United States of America. 2006;103(3):732-
533 7. Epub 2006/01/13. doi: 10.1073/pnas.0506655103. PubMed PMID: 16407106;
534 PubMed Central PMCID: PMC1334644.
- 535 7. Huang BR, Tsai CF, Lin HY, Tseng WP, Huang SS, Wu CR, et al. Interaction
536 of inflammatory and anti-inflammatory responses in microglia by *Staphylococcus*
537 *aureus*-derived lipoteichoic acid. Toxicology and applied pharmacology.
538 2013;269(1):43-50. Epub 2013/03/19. doi: 10.1016/j.taap.2013.03.004. PubMed
539 PMID: 23500011.
- 540 8. Correa P. Human gastric carcinogenesis: a multistep and multifactorial
541 process--First American Cancer Society Award Lecture on Cancer Epidemiology and
542 Prevention. Cancer research. 1992;52(24):6735-40. Epub 1992/12/15. PubMed
543 PMID: 1458460.
- 544 9. Ziebarth D, Spiegelhalder B, Bartsch H. N-nitrosation of medicinal drugs
545 catalysed by bacteria from human saliva and gastro-intestinal tract, including
546 *Helicobacter pylori*. Carcinogenesis. 1997;18(2):383-9. Epub 1997/02/01. PubMed
547 PMID: 9054633.
- 548 10. Biarc J, Nguyen IS, Pini A, Gosse F, Richert S, Thierse D, et al. Carcinogenic
549 properties of proteins with pro-inflammatory activity from *Streptococcus infantarius*
550 (formerly *S.bovis*). Carcinogenesis. 2004;25(8):1477-84. Epub 2004/01/27. doi:
551 10.1093/carcin/bgh091. PubMed PMID: 14742316.
- 552 11. Brestoff JR, Artis D. Commensal bacteria at the interface of host metabolism
553 and the immune system. Nature immunology. 2013;14(7):676-84. doi:
554 10.1038/ni.2640. PubMed PMID: 23778795; PubMed Central PMCID: PMC4013146.

- 555 12. Catsburg CE, Gago-Dominguez M, Yuan JM, Castelao JE, Cortessis VK, Pike
556 MC, et al. Dietary sources of N-nitroso compounds and bladder cancer risk: Findings
557 from the Los Angeles bladder cancer study. *International journal of cancer Journal*
558 *international du cancer*. 2013. Epub 2013/06/19. doi: 10.1002/ijc.28331. PubMed
559 PMID: 23775870.
- 560 13. Keszei AP, Goldbohm RA, Schouten LJ, Jakszyn P, van den Brandt PA.
561 Dietary N-nitroso compounds, endogenous nitrosation, and the risk of esophageal
562 and gastric cancer subtypes in the Netherlands Cohort Study. *The American journal*
563 *of clinical nutrition*. 2013;97(1):135-46. Epub 2012/11/30. doi:
564 10.3945/ajcn.112.043885. PubMed PMID: 23193003.
- 565 14. Salter SJ, Cox MJ, Turek EM, Calus ST, Cookson WO, Moffatt MF, et al.
566 Reagent and laboratory contamination can critically impact sequence-based
567 microbiome analyses. *BMC biology*. 2014;12:87. Epub 2014/11/13. doi:
568 10.1186/s12915-014-0087-z. PubMed PMID: 25387460; PubMed Central PMCID:
569 PMC4228153.
- 570 15. Manichanh C, Rigottier-Gois L, Bonnaud E, Gloux K, Pelletier E, Frangeul L,
571 et al. Reduced diversity of faecal microbiota in Crohn's disease revealed by a
572 metagenomic approach. *Gut*. 2006;55(2):205-11. doi: 10.1136/gut.2005.073817.
573 PubMed PMID: WOS:000234553500016.
- 574 16. Li TH, Qin Y, Sham PC, Lau KS, Chu KM, Leung WK. Alterations in Gastric
575 Microbiota After H. Pylori Eradication and in Different Histological Stages of Gastric
576 Carcinogenesis. *Scientific reports*. 2017;7:44935. Epub 2017/03/23. doi:
577 10.1038/srep44935. PubMed PMID: 28322295.

- 578 17. Gao Z, Guo B, Gao R, Zhu Q, Qin H. Microbiota disbiosis is associated with
579 colorectal cancer. *Front Microbiol.* 2015;6:20. doi: 10.3389/fmicb.2015.00020.
580 PubMed PMID: 25699023; PubMed Central PMCID: PMC4313696.
- 581 18. Nakae H, Tsuda A, Matsuoka T, Mine T, Koga Y. Gastric microbiota in the
582 functional dyspepsia patients treated with probiotic yogurt. *BMJ Open Gastroenterol.*
583 2016;3(1):e000109. doi: 10.1136/bmjgast-2016-000109. PubMed PMID: 27752337.
- 584 19. von Rosenvinge EC, Song Y, White JR, Maddox C, Blanchard T, Fricke WF.
585 Immune status, antibiotic medication and pH are associated with changes in the
586 stomach fluid microbiota. *The ISME journal.* 2013;7(7):1354-66. Epub 2013/03/08.
587 doi: 10.1038/ismej.2013.33. PubMed PMID: 23466701; PubMed Central PMCID:
588 PMC3695299.
- 589 20. Paroni Sterbini F, Palladini A, Masucci L, Cannistraci CV, Pastorino R, Ianaro
590 G, et al. Effects of Proton Pump Inhibitors on the Gastric Mucosa-Associated
591 Microbiota in Dyspeptic Patients. *Applied and environmental microbiology.*
592 2016;82(22):6633-44. Epub 2016/10/30. doi: 10.1128/AEM.01437-16. PubMed
593 PMID: 27590821; PubMed Central PMCID: PMC5086557.
- 594 21. Jackson MA, Goodrich JK, Maxan ME, Freedberg DE, Abrams JA, Poole AC,
595 et al. Proton pump inhibitors alter the composition of the gut microbiota. *Gut.*
596 2016;65(5):749-56. doi: 10.1136/gutjnl-2015-310861. PubMed PMID: 26719299;
597 PubMed Central PMCID: PMC4853574.
- 598 22. Schulz C, Schutte K, Koch N, Vilchez-Vargas R, Wos-Oxley ML, Oxley AP, et
599 al. The active bacterial assemblages of the upper GI tract in individuals with and
600 without *Helicobacter* infection. *Gut.* 2016. Epub 2016/12/07. doi: 10.1136/gutjnl-
601 2016-312904. PubMed PMID: 27920199.

- 602 23. Martin ME, Bhatnagar S, George MD, Paster BJ, Canfield DR, Eisen JA, et al.
603 The impact of *Helicobacter pylori* infection on the gastric microbiota of the rhesus
604 macaque. PLoS One. 2013;8(10):e76375. doi: 10.1371/journal.pone.0076375.
605 PubMed PMID: 24116104; PubMed Central PMCID: PMC3792980.
- 606 24. Eun CS, Kim BK, Han DS, Kim SY, Kim KM, Choi BY, et al. Differences in
607 Gastric Mucosal Microbiota Profiling in Patients with Chronic Gastritis, Intestinal
608 Metaplasia, and Gastric Cancer Using Pyrosequencing Methods. *Helicobacter*.
609 2014;19(6):407-16. doi: Doi 10.1111/Hel.12145. PubMed PMID:
610 WOS:000345305700001.
- 611 25. Farrell JJ, Zhang L, Zhou H, Chia D, Elashoff D, Akin D, et al. Variations of
612 oral microbiota are associated with pancreatic diseases including pancreatic cancer.
613 Gut. 2012;61(4):582-8. doi: 10.1136/gutjnl-2011-300784. PubMed PMID: 21994333;
614 PubMed Central PMCID: PMC3705763.
- 615 26. Muto M, Hitomi Y, Ohtsu A, Shimada H, Kashiwase Y, Sasaki H, et al.
616 Acetaldehyde production by non-pathogenic *Neisseria* in human oral microflora:
617 implications for carcinogenesis in upper aerodigestive tract. International journal of
618 cancer Journal international du cancer. 2000;88(3):342-50. PubMed PMID:
619 11054661.
- 620 27. Khosravi Y, Dieye Y, Loke MF, Goh KL, Vadivelu J. Streptococcus mitis
621 Induces Conversion of *Helicobacter pylori* to Coccoid Cells during Co-Culture In
622 Vitro. PLoS One. 2014;9(11):e112214. Epub 2014/11/12. doi:
623 10.1371/journal.pone.0112214. PubMed PMID: 25386948; PubMed Central PMCID:
624 PMC4227722.

625 28. Chan WY, Hui PK, Leung KM, Chow J, Kwok F, Ng CS. Coccoid forms of
626 *Helicobacter pylori* in the human stomach. *American journal of clinical pathology*.
627 1994;102(4):503-7. Epub 1994/10/01. PubMed PMID: 7524304.

628 29. Li N, Han L, Chen J, Lin X, Chen H, She F. Proliferative and apoptotic effects
629 of gastric epithelial cells induced by coccoid *Helicobacter pylori*. *Journal of basic*
630 *microbiology*. 2013;53(2):147-55. Epub 2012/05/15. doi: 10.1002/jobm.201100370.
631 PubMed PMID: 22581720.

632 30. Kim HS, Lee HE, Yang HK, Kim WH. High lactate dehydrogenase 5
633 expression correlates with high tumoral and stromal vascular endothelial growth
634 factor expression in gastric cancer. *Pathobiology*. 2014;81(2):78-85. doi:
635 10.1159/000357017. PubMed PMID: 24401755.

636 31. Wang J, Yuan W, Chen Z, Wu S, Chen J, Ge J, et al. Overexpression of
637 G6PD is associated with poor clinical outcome in gastric cancer. *Tumour Biol*.
638 2012;33(1):95-101. doi: 10.1007/s13277-011-0251-9. PubMed PMID: 22012600.

639 32. Lancaster CR, Kroger A, Auer M, Michel H. Structure of fumarate reductase
640 from *Wolinella succinogenes* at 2.2 Å resolution. *Nature*. 1999;402(6760):377-85.
641 doi: 10.1038/46483. PubMed PMID: 10586875.

642 33. Ge Z. Potential of fumarate reductase as a novel therapeutic target in
643 *Helicobacter pylori* infection. *Expert Opin Ther Targets*. 2002;6(2):135-46. doi:
644 10.1517/14728222.6.2.135. PubMed PMID: 12223076.

645 34. Kassem, II, Khatri M, Sanad YM, Wolboldt M, Saif YM, Olson JW, et al. The
646 impairment of methylmenaquinol:fumarate reductase affects hydrogen peroxide
647 susceptibility and accumulation in *Campylobacter jejuni*. *Microbiologyopen*.
648 2014;3(2):168-81. doi: 10.1002/mbo3.158. PubMed PMID: 24515965; PubMed
649 Central PMCID: PMC3996566.

650 35. Wang YM, Gu ML, Ji F. Succinate dehydrogenase-deficient gastrointestinal
651 stromal tumors. *World J Gastroenterol*. 2015;21(8):2303-14. doi:
652 10.3748/wjg.v21.i8.2303. PubMed PMID: 25741136; PubMed Central PMCID:
653 PMCPMC4342905.

654 36. Coulton GR, Firth JA. Cytochemical evidence for functional zonation of
655 parietal cells within the gastric glands of the mouse. *Histochem J*. 1983;15(11):1141-
656 50. PubMed PMID: 6317615.

657 37. Kumar JD, Steele I, Moore AR, Murugesan SV, Rakonczay Z, Venglovecz V,
658 et al. Gastrin stimulates MMP-1 expression in gastric epithelial cells: putative role in
659 gastric epithelial cell migration. *American journal of physiology Gastrointestinal and*
660 *liver physiology*. 2015;309(2):G78-86. Epub 2015/05/16. doi:
661 10.1152/ajpgi.00084.2015. PubMed PMID: 25977510; PubMed Central PMCID:
662 PMC4504956.

663 38. Moore AR, Boyce M, Steele IA, Campbell F, Varro A, Pritchard DM.
664 Netazepide, a gastrin receptor antagonist, normalises tumour biomarkers and
665 causes regression of type 1 gastric neuroendocrine tumours in a nonrandomised trial
666 of patients with chronic atrophic gastritis. *PLoS One*. 2013;8(10):e76462. doi:
667 10.1371/journal.pone.0076462. PubMed PMID: 24098507; PubMed Central PMCID:
668 PMC3788129.

669 39. Boyce M, Moore AR, Sagatun L, Parsons BN, Varro A, Campbell F, et al.
670 Netazepide, a gastrin/cholecystokinin-2 receptor antagonist, can eradicate gastric
671 neuroendocrine tumours in patients with autoimmune chronic atrophic gastritis.
672 *British journal of clinical pharmacology*. 2016. Epub 2016/10/06. doi:
673 10.1111/bcp.13146. PubMed PMID: 27704617.

40. Dixon MF, Genta RM, Yardley JH, Correa P. Classification and grading of gastritis. The updated Sydney System. International Workshop on the Histopathology of Gastritis, Houston 1994. Am J Surg Pathol. 1996;20(10):1161-81. PubMed PMID: 8827022.
41. TRI-Reagent®. Extraction Protocol. <http://www.sigmaaldrich.com/technical-documents/protocols/biology/tri-reagent.html> Accessed 16/12/15.
42. Dockray GJ. Immunochemical studies on big gastrin using NH₂-terminal specific antisera. Regulatory peptides. 1980;1(3):169-86. Epub 1980/12/01. PubMed PMID: 6165051.
43. Varro A, Ardill JE. Gastrin: an analytical review. Annals of clinical biochemistry. 2003;40(Pt 5):472-80. Epub 2003/09/25. doi: 10.1258/000456303322326380. PubMed PMID: 14503984.
44. Laufer AS, Metlay JP, Gent JF, Fennie KP, Kong Y, Pettigrew MM. Microbial communities of the upper respiratory tract and otitis media in children. mBio. 2011;2(1):e00245-10. Epub 2011/02/03. doi: 10.1128/mBio.00245-10. PubMed PMID: 21285435; PubMed Central PMCID: PMC3031303.

Supporting Information Legend:

Supplementary Methods_15.06.17_PLOSP.docx includes complete details of the structure of mock bacterial communities, and sequencing and statistical methods

FIGURE LEGENDS

Table 1. Summary of patient group characteristics. ND = Not done, IQR =

Interquartile range, 25% and 75%.

Figure 1. (A) Median fasting serum gastrin concentrations (pM) in patient groups.

Kruskal-Wallis test with Dunn's comparison, plotted using Tukey's method $^*=P<0.05$,

and $^{****}=P<0.0001$ vs control. (B) Mean number of OTUs identified within each

patient group, 1-way ANOVA and Tukey's multiple comparison test $^*=P<0.05$,

$^{**}=P<0.01$, Control vs Autoimmune atrophic gastritis $P=0.059$, Control vs Neg

$P=0.061$ and Hp-induced atrophic gastritis vs Neg $P=0.059$.

Figure 2. Five different diversity indices of human gastric microbiota (Fisher alpha:

parametric index of diversity that models species as logseries distribution; Pielou's

evenness: how close in numbers each species is; Richness: number of species per

sample; Shannon: a commonly used index to characterise species diversity; and

Simpson: which takes into account the number of species present, as well as their

relative abundance). Pair-wise ANOVA was performed between different groups and

if significant ($P<0.001$), the p-values have been drawn on top. Atrophy=*H. pylori*

associated atrophy, Auto=autoimmune atrophic gastritis, Control=normal stomach,

HP Gast=*H. pylori* associated gastritis, PPI=proton pump inhibitor and Neg=

extraction control.

Figure 3. Relative abundances of taxa found within (A) groups and (B) individual

human gastric biopsies. Hp=*H. pylori*, IM=intestinal metaplasia, IM+At=intestinal

metaplasia and atrophy, PPI=proton pump inhibitor, EC=extraction controls (one of

the EC samples was included in a run with more *H. pylori* dominant samples),

H=H₂O and M=mock community (which showed consistent findings on two runs as

shown). All *H. pylori* atrophic gastritis samples were positive for *H. pylori* by serology, + indicates whether these samples were also positive by histology/rapid urease test. Autoimmune atrophic gastritis samples recorded as 's' were also positive for *H. pylori* by serology.

Figure 4. Nonmetric distance scaling (NMDS) demonstrating clustering of patient groups using (A) unweighted Unifrac distance (pair-wise distance between samples is calculated as a normalised difference in cumulative branch lengths of the observed OTUs for each sample on the phylogenetic tree without taking into account their abundances in samples), (B) Bray-Curtis distance (abundance of OTUs alone and not considering the phylogenetic distance) and (C) weighted Unifrac (unweighted unifrac distance weighted by abundances of OTUs). Serum gastrin concentration indicated by size of each point. Ellipses represent 95% CI of standard error for a given group. Dotted ellipses represent the 95% CI of standard error when *H. pylori* were removed from the analysis. Atrophy=*H. pylori* associated atrophic gastritis, Auto=autoimmune atrophic gastritis, Control=normal, HP Gastr=*H. pylori* associated gastritis and PPI=proton pump inhibitor. PERMANOVA (distances against groups) suggests significant differences ($P < 0.001$ for all three distances) in microbial community explaining the following variations (R^2) between groups: 10% (8.6% without *H. pylori* when using Unweighted Unifrac; 58% (14.5% without *H. pylori*) when using Weighted Unifrac; and 15% when using Bray-Curtis distance. No significant explanation was observed ($P > 0.05$) for age, BMI, or serum gastrin concentration in the PERMANOVA test. (D) Data from betadisper plots (a mean to compare the spread/variability of samples for different groups) representing difference in distances (Bray-Curtis, Unweighted and weighted Unifrac) of group members from the centre/mean of individual groups after obtaining a reduced-order

representation of abundance table using Principle Coordinate Analysis. The pair-wise differences in distances from group centre/mean were then subjected to ANOVA and if significant ($P < 0.001$), the p-values were drawn on top.

Figure 5. Co-occurrence network analysis between different genera (OTUs collated together at genus level) when considering samples for (A) normal stomach, (B) *H. pylori* gastritis, (C) *H. pylori*-induced atrophic gastritis and (D) autoimmune atrophic gastritis. The genera were connected (Blue: positive correlation; Red: negative correlation) when the pair-wise correlation values were significant ($P_{adj} < 0.05$) after adjusting the P values for multiple comparisons. Furthermore, subcommunity detection was performed by placing the genera in the same subcommunity (represented by colour of nodes) when many links were found at correlation values > 0.75 between members of the subcommunity. The size of the nodes represent the degree of connections.

Supplementary Figure and Table Legends

Figure S1. Relative abundances of taxa found within human gastric biopsies after removal of Helicobacteraceae. Hp=*H. pylori*, IM=intestinal metaplasia, IM+At=intestinal metaplasia and atrophy, PPI=proton pump inhibitor. All *H. pylori* atrophy samples were positive for *H. pylori* by serology.

Figure S3. Co-occurrence network analysis between different genera (OTUs collated together at genus level) when considering samples for (A) PPI. The genera were connected (Blue: positive correlation; Red: negative correlation) when the pair-wise correlation values were significant ($P_{adj} < 0.05$) after adjusting the P values for

multiple comparisons. Furthermore, subcommunity detection was performed by placing the genera in the same subcommunity (represented by colour of nodes) when many links were found at correlation values >0.75 between members of the subcommunity. The size of the nodes represent the degree of connections (B) network-wide statistics by degree, closeness, betweenness and eigenvalue centrality for *H. pylori* atrophic gastritis cases. The nodes (coloured with respect to subcommunity they are part of) were placed on concentric circles with values increasing from center to the periphery. A high betweenness for a node suggests many connections, whereas a high eigenvalue centrality suggests that those connections, in turn, are all well connected. On average a high betweenness and at the same time low eigenvalue centrality for a subcommunity suggests a keystone/important subcommunity.

Figure S4. Mean updated Sydney scores in antrum and corpus. Updated Sydney scores were the sum of the scores for 5 individual parameters each scored 0-3 [40]. **** $p < 0.0001$ versus control from the same mucosal site by 2-way ANOVA using Dunnett's multiple comparison test.

Table S1. Significantly different genera identified between normal stomach samples and PPI, autoimmune atrophic gastritis, *H. pylori*-induced atrophic gastritis and *H. pylori* gastritis. The most significant species are identified at the top. Differential expression analysis based on the Negative Binomial (Gamma-Poisson) distribution and were corrected for multiple comparisons. * indicates a genus no longer significant when *H. pylori* was removed from the analysis.

Table S2A. Stable bacterial populations and correlations in PPI patients compared to other groups (if the correlation between two genera were consistently positive or

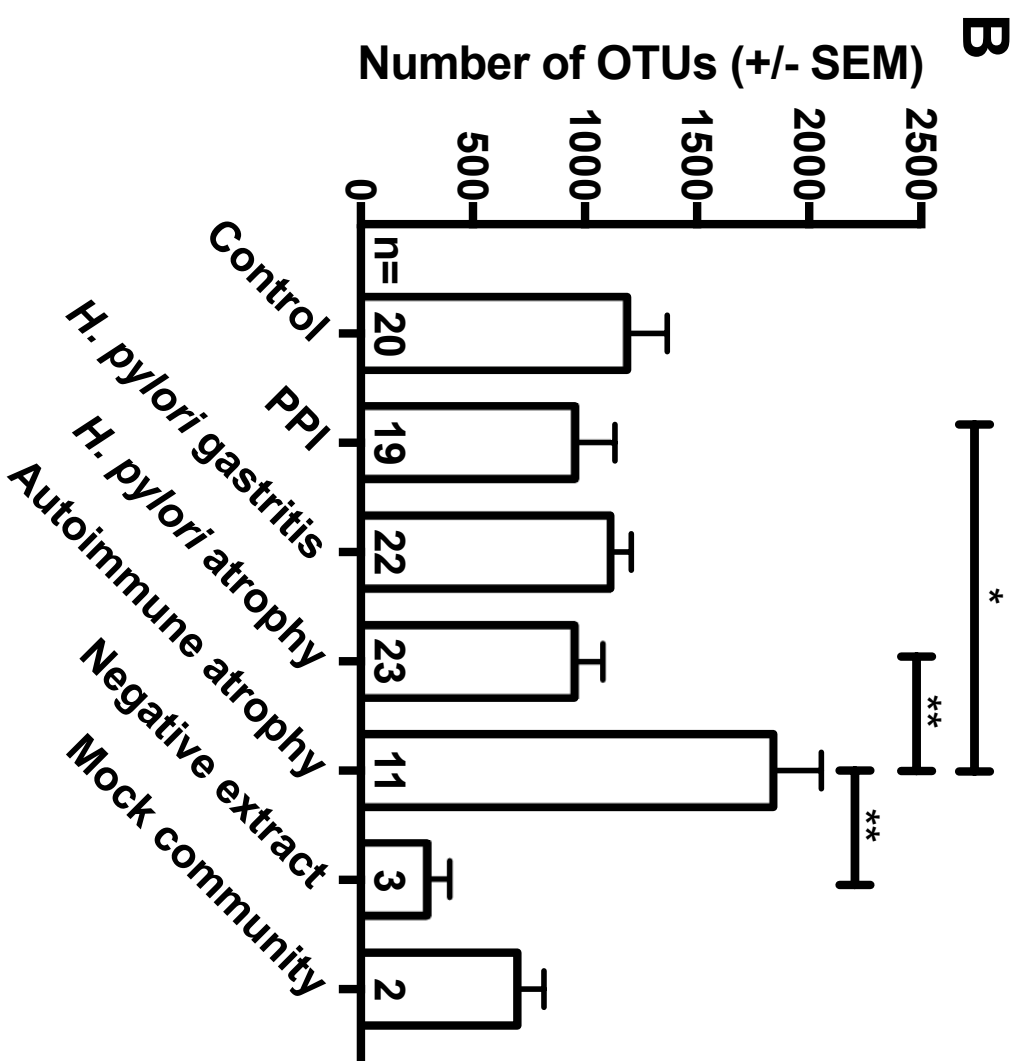
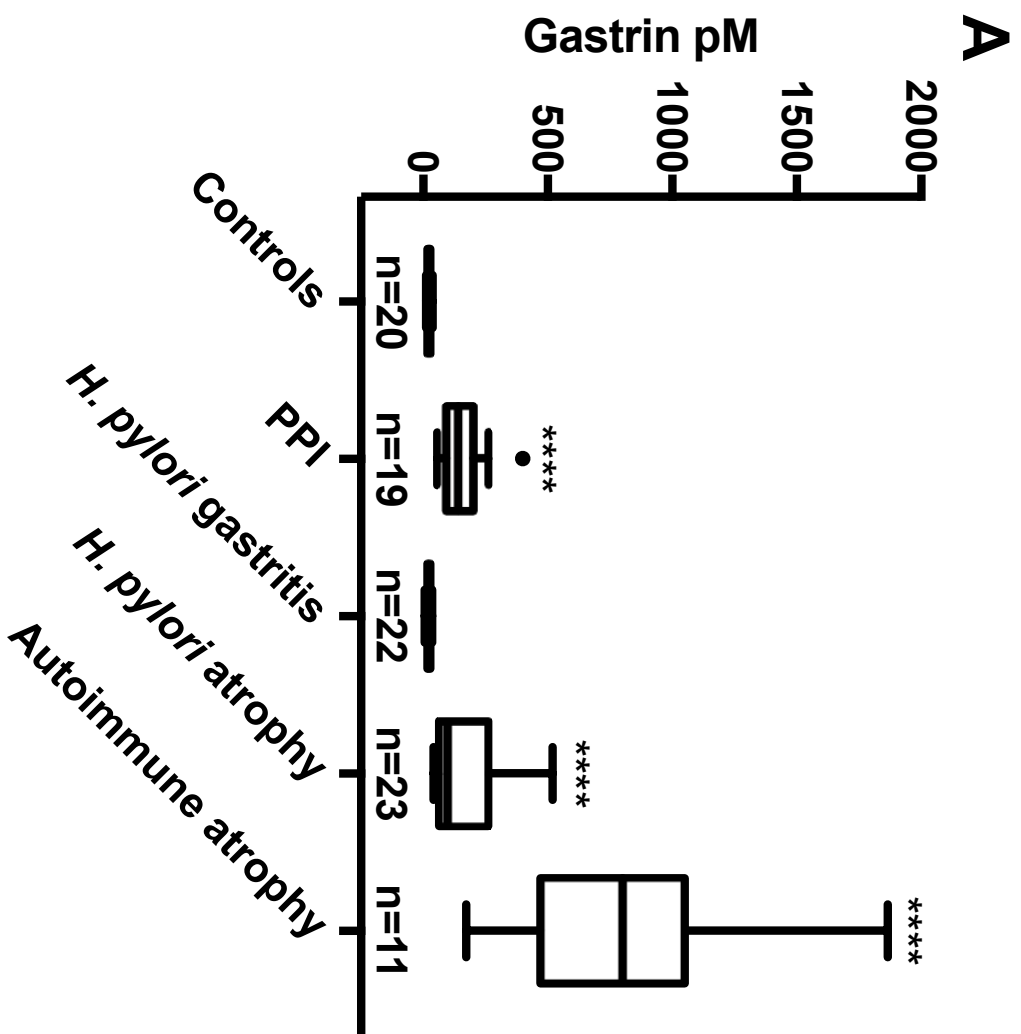
negative in different groups). PPI versus *H. pylori*-induced atrophic gastritis in table S2B. No significant comparisons were found between PPI and autoimmune atrophic gastritis groups.

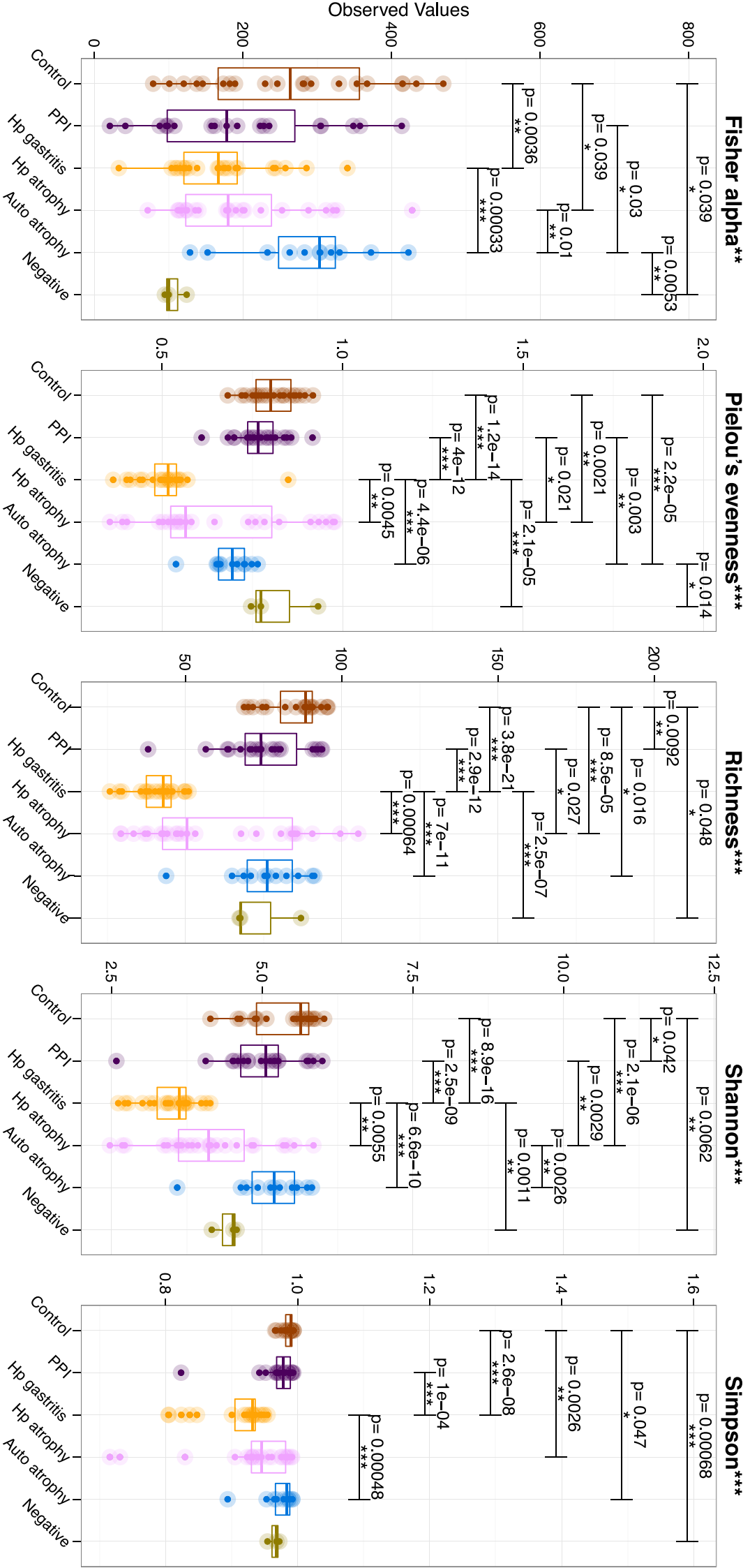
Table S2B. Stable bacterial populations and correlations in *H. pylori*-induced atrophic gastritis patients compared to other groups.

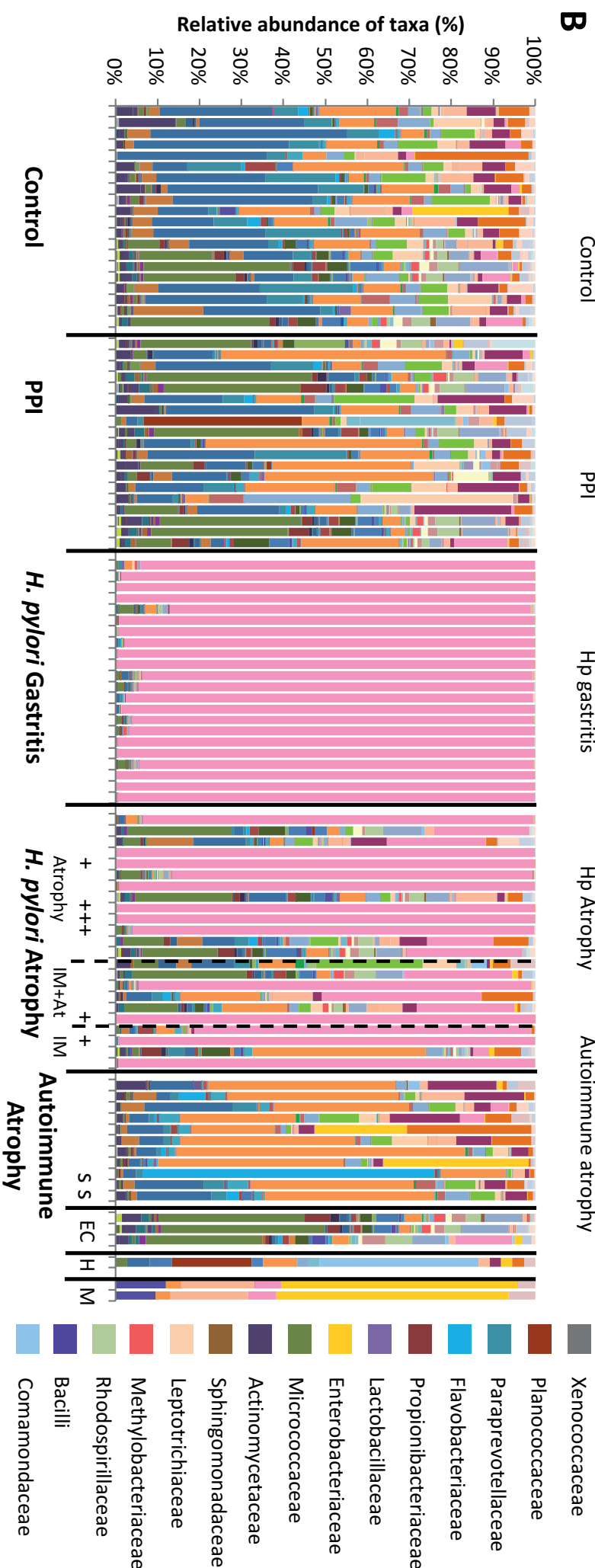
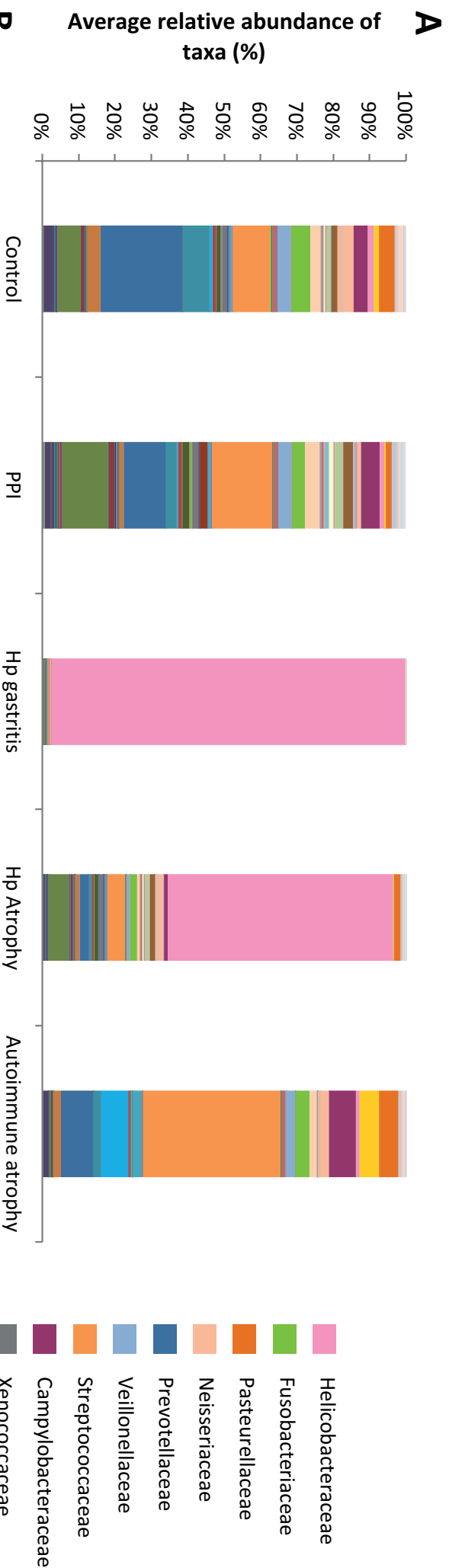
Table S3. The top most significant predicted pathways found for each group comparison.

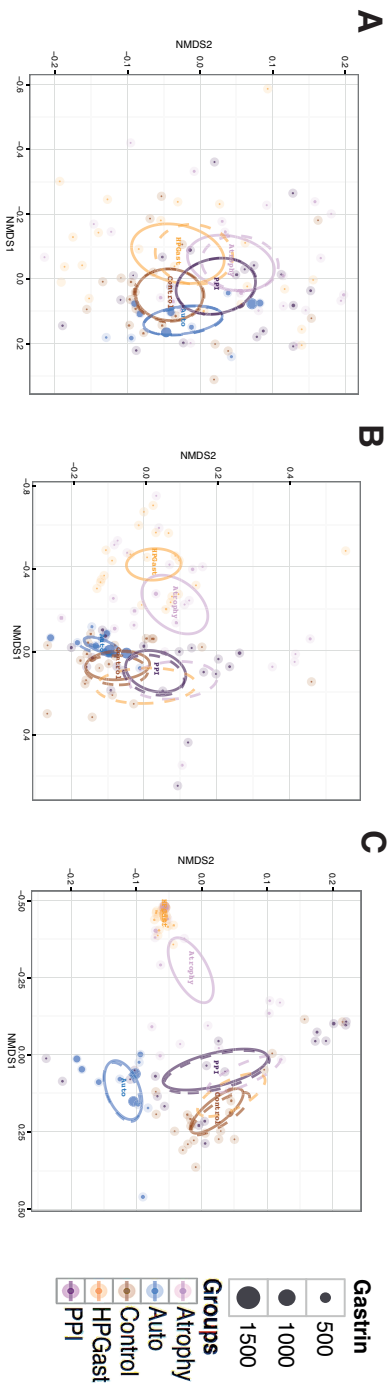
Table S4A. Significant bacterial species identified between *H. pylori* atrophic gastritis and *H. pylori* gastritis. The most significant species are identified at the top. Differential expression analysis based on the Negative Binomial (Gamma-Poisson) distribution. Streptococcus identified by BLAST as *S. mitis* with 98% coverage, 99% identity and *Neisseria mucosa* had 98% coverage and 100% identity. None of these OTUs remained significant when *H. pylori* was removed from the analysis.

Table S4B. Significant bacterial genera identified between autoimmune atrophic gastritis and *H. pylori*-induced atrophic gastritis. The most significant species are identified at the top. Differential expression analysis based on the Negative Binomial (Gamma-Poisson) distribution. NB when *H. pylori* was removed from the analysis these genera remained significant, with an additional genus *Desulfobulbus* also reaching significance.



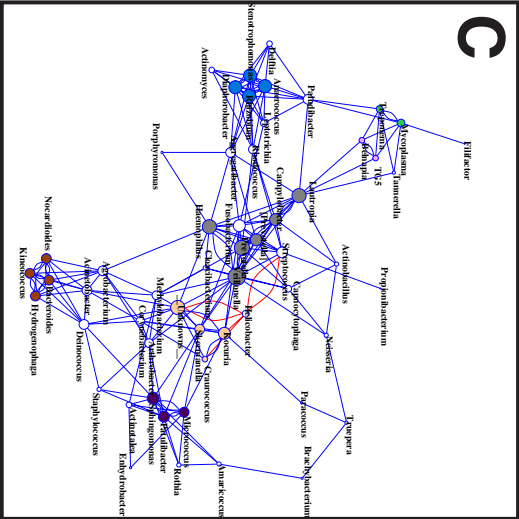
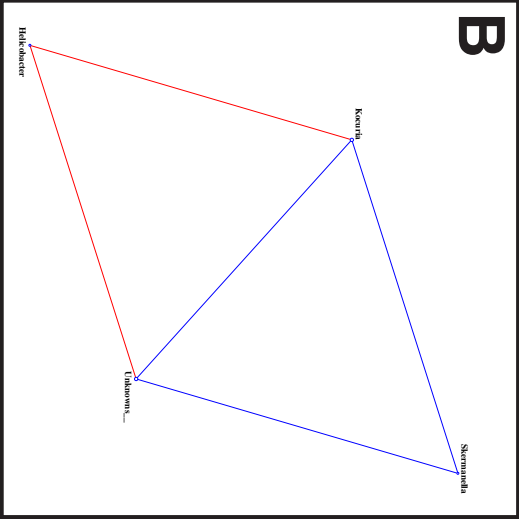
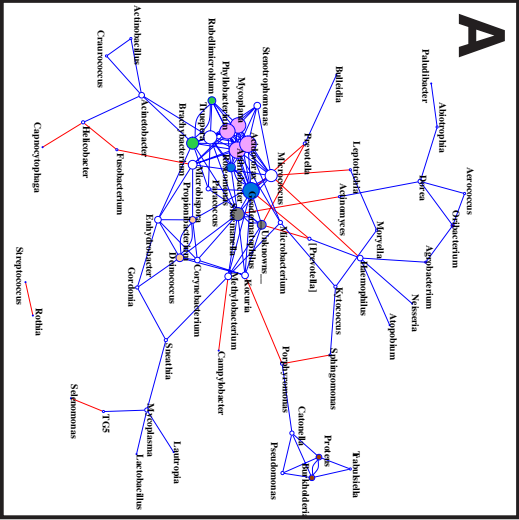






D

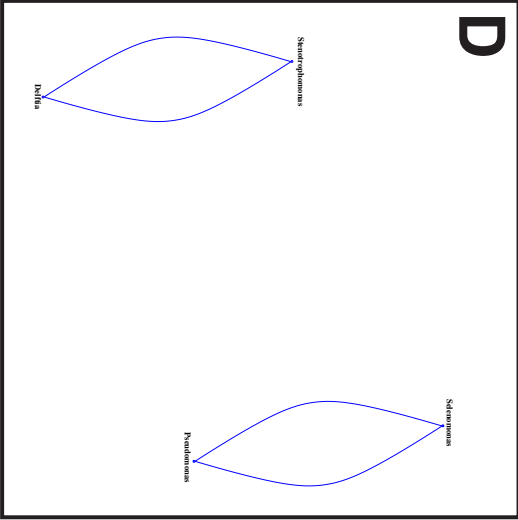
		<i>H. pylori</i> included in analysis			<i>H. pylori</i> removed from analysis		
Group Comparison		Unifrac significance (presence/absence)	Bray-Curtis significance (abundance)	Weighted Unifrac (abundance)	Unifrac significance (presence/absence)	Bray-Curtis significance (abundance)	Weighted Unifrac (abundance)
Control	PPI	ns	ns	0.0116 *	ns	ns	0.0132 *
	HP Gastritis	ns	0.0270 *	1.3741×10^{-12} ***	ns	ns	ns
	HP Atrophy	0.059	ns	ns	ns	0.0193 *	ns
PPI	Autoimmune	0.0638	ns	ns	0.0564	ns	ns
	HP Gastritis	ns	0.0008 ***	9.9989×10^{-25} ***	ns	ns	ns
	HP Atrophy	ns	ns	ns	ns	ns	ns
HP Gastritis	Autoimmune	0.0019 **	0.004 **	0.0037 **	0.0018 **	0.0043 **	0.0034 **
	HP Atrophy	ns	0.0080 **	4.1694×10^{-16} ***	ns	ns	ns
	Autoimmune	0.0060 **	ns	2.5084×10^{-9} ***	0.0090 **	0.0249 *	0.0233 *
HP Atrophy	Autoimmune	3.159×10^{-5} ***	ns	0.0568	1.191×10^{-4} ***	3.765×10^{-4} ***	0.0227 *



Normal

H. pylori gastritis

H. pylori atrophy



Autoimmune atrophy